2018

Three distinct sets of connector hubs integrate human brain function

Evan M. Gordon
VISN 17 Center of Excellence for Research on Returning War Veterans

Charles J. Lynch
Georgetown University

Caterina Gratton
Washington University School of Medicine in St. Louis

Timothy O. Laumann
Washington University School of Medicine in St. Louis

Adrian W. Gilmore
Washington University School of Medicine in St. Louis

See next page for additional authors

Report

Cell Reports

Three Distinct Sets of Connector Hubs Integrate Human Brain Function

Graphical Abstract

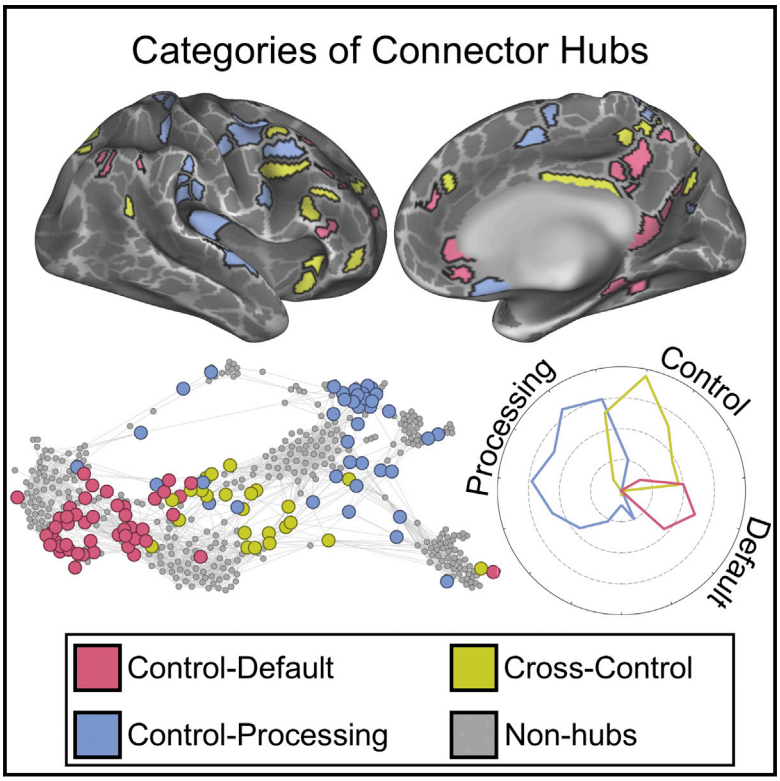

Authors

Evan M. Gordon, Charles J. Lynch, Caterina Gratton, ..., Steven E. Petersen, Nico U.F. Dosenbach, Steven M. Nelson

Correspondence

evan.gordon@va.gov

In Brief

Gordon et al. identify separable control-processing, control-default, and cross-control connector hubs that integrate specific brain networks. These hub sets are differentially engaged during task performance and affect networks differently when artificially lesioned. Different connector hub sets may separately enable top-down control of sensory motor, emotional, and control of control functions.

Highlights

- Three dissociable hub categories integrate networked brain function in humans
- Control-processing, cross-control, and control-default hubs link different networks
- Simulated lesions of each hub category isolate those linked brain networks
- Task activation differs by hub category even when it does not differ by network

Gordon et al., 2018, Cell Reports *24*, 1687–1695
August 14, 2018
https://doi.org/10.1016/j.celrep.2018.07.050

CellPress

Cell Reports
Report

Three Distinct Sets of Connector Hubs Integrate Human Brain Function

Evan M. Gordon,[1,2,3,15,*] Charles J. Lynch,[4,14] Caterina Gratton,[5] Timothy O. Laumann,[5] Adrian W. Gilmore,[6,13] Deanna J. Greene,[7,12] Mario Ortega,[5] Annie L. Nguyen,[5] Bradley L. Schlaggar,[5,7,8,11,12] Steven E. Petersen,[5,6,7,8,9] Nico U.F. Dosenbach,[5,10,11] and Steven M. Nelson[1,2,3]

[1]VISN 17 Center of Excellence for Research on Returning War Veterans, Waco, TX 76711, USA
[2]Center for Vital Longevity, School of Behavioral and Brain Sciences, University of Texas at Dallas, Dallas, TX 75235, USA
[3]Department of Psychology and Neuroscience, Baylor University, Waco, TX 76789, USA
[4]Department of Psychology, Georgetown University, Washington, DC 20057, USA
[5]Department of Neurology, Washington University in St. Louis, St. Louis, MO 63110, USA
[6]Department of Psychological and Brain Sciences, Washington University in St. Louis, St. Louis, MO 63110, USA
[7]Department of Radiology, Washington University in St. Louis, St. Louis, MO 63110, USA
[8]Department of Neuroscience, Washington University in St. Louis, St. Louis, MO 63110, USA
[9]Department of Biomedical Engineering, Washington University in St. Louis, St. Louis, MO 63110, USA
[10]Department of Occupational Therapy, Washington University in St. Louis, St. Louis, MO 63110, USA
[11]Department of Pediatrics, Washington University in St. Louis, St. Louis, MO 63110, USA
[12]Department of Psychiatry, Washington University in St. Louis, St. Louis, MO 63110, USA
[13]Laboratory of Brain and Cognition, National Institute of Mental Health, NIH, Bethesda, MD 20892, USA
[14]Feil Family Brain and Mind Research Institute, Weill Cornell Medical College, New York, NY 10065, USA
[15]Lead Contact
*Correspondence: evan.gordon@va.gov
https://doi.org/10.1016/j.celrep.2018.07.050

SUMMARY

Control over behavior is enabled by the brain's control networks, which interact with lower-level sensory motor and default networks to regulate their functions. Such interactions are facilitated by specialized "connector hub" regions that interconnect discrete networks. Previous work has treated hubs as a single category of brain regions, although their unitary nature is dubious when examined in individual brains. Here we investigated the nature of hubs by using fMRI to characterize individual-specific hub regions in two independent datasets. We identified three separable sets of connector hubs that integrate information between specific brain networks. These three hub categories occupy different positions within the brain's network structure; they affect networks differently when artificially lesioned, and they are differentially engaged during cognitive and motor task performance. This work suggests a model of brain organization in which different connector hubs integrate control functions and enable top-down control of separate processing streams.

INTRODUCTION

Complex behavior in humans is enabled by the networked interaction of multiple brain regions specialized for specific behavioral functions. Although some of these regions are related to low-level sensory and motor functions, other regions, primarily in the prefrontal and parietal cortex, exhibit strong activity only during performance of complex cognitive tasks (Dosenbach et al., 2006; Duncan and Owen, 2000). These regions are argued to interact with the low-level processing systems and, by that interaction, enable flexible, top-down control over behavior that is dynamically modified according to the moment-to-moment demands of the environment (Posner and Petersen, 1990; Power and Petersen, 2013).

Using an fMRI technique called resting state functional connectivity (RSFC), these "control" regions are separable into at least two (Dosenbach et al., 2007, 2008) and as many as five (Power and Petersen, 2013) distinct brain networks, each of which exhibits coordinated activity within the network but comparatively little interaction between networks. In combination, these control networks interact with lower-level systems that include "processing" systems that represent external stimuli (somatosensory, visual, and auditory) and motor outputs, as well as systems representing internal information stores (memories, emotions, and semantics). These systems also exist as separable brain networks (Power et al., 2011; Yeo et al., 2011), and interaction between various networks increases during performance of more complex cognitive tasks (Cole et al., 2013; Mattar et al., 2015; Shine et al., 2016), which is associated with better task performance (Shine et al., 2016). The specific mechanisms by which control and lower-level networks interact to enable complex cognition are an area of intense interest (van den Heuvel and Sporns, 2013).

One compelling concept borrowed from the field of network science is that interactions between networks may be enabled by specialized network nodes (here, brain regions), termed "connector hubs," that link networks together (Guimerà et al., 2007). Previous work has confirmed that brain networks do contain diversely connected hubs (Bertolero et al., 2017; Power et al., 2013) that are strongly engaged (Bertolero et al., 2015) and

strongly link different networks (Cohen and D'Esposito, 2016; Cole et al., 2013; Gratton et al., 2016) during task performance. Disruption of brain hubs by lesions (Gratton et al., 2012) or by transcranial magnetic stimulation (TMS) (Lynch et al., 2018) causes alteration of brain network function and widespread degradation of cognitive function (Warren et al., 2014). Together, this evidence points to connector hubs as critical regions enabling the interaction of control and processing networks for complex cognitive function (Gratton et al., 2018). Thus, connector hubs likely represent regions analogous to the transmodal "network epicenters" described by Mesulam (1998) as providing top-down influence over lower-level networks.

Previously, connector hubs have been conceptualized as a single category of brain regions—a "diverse club" that serves as an interconnected core, allowing integration across networks (Bertolero et al., 2017). Such characterizations are derived from data averaged across groups (Bertolero et al., 2015, 2017; Gratton et al., 2016; Power et al., 2013). However, inter-individual spatial variability of brain networks may artificially induce the appearance of interconnected regions in group data (Gordon et al., 2017). By contrast, examination of brain networks in single individuals indicates a different organization: functional networks are connected—likely via connector hubs—to specific subsets of other networks, not to a single core of brain regions (Gordon et al., 2017). This finding suggests that connector hubs are not uniform in their functional properties; rather, different hubs may link different subsets of control and processing networks to enable different functions. This organization would converge with Mesulam's concept of network epicenters providing process-specific regulatory control (Mesulam, 1998). If true, characterizing organizational and functional distinctions between hubs would be a major step forward in understanding the role these key regions play in human behavior.

Here we used RSFC to identify hubs in individual human brains. We characterized each hub based on its network connectivity, and we clustered hubs across individuals into discrete sets with different connectivity profiles. We then described the connectivity, spatial distribution, and position in network space of each set of hubs, and we characterized the effects of removing hub sets (i.e., creating artificial lesions) on the brain's network structure. Finally, we examined whether a hub's set was related to its activation during task performance. These analyses employed the Midnight Scan Club (MSC) data, a dataset of 10 subjects with more than 10 hr of fMRI data each (Gordon et al., 2017). We replicated all results using a subset of the Human Connectome Project (HCP) dataset (n = 80, 1 hr/subject; Van Essen et al., 2012). Based on previous work conceptualizing hubs as enabling top-down control of process-specific lower-level systems (Cole et al., 2013; Gratton et al., 2018), we hypothesized that hubs would dissociate into separate categories, reflecting links between control networks and process-specific systems.

RESULTS

Connector Hubs Cluster into Three Discrete Categories

In each subject, an individual-specific cortical parcellation was created (Gordon et al., 2016). Parcel network identities were defined in each subject (following Gordon et al., 2017). Networks included dorsal attention (DAN), fronto-parietal (FPN), parietal memory (PMN), salience (Sal), default mode (DMN), contextual association (CAN), ventral attention (VAN), medial visual (mVis), lateral visual (lVis), leg somatomotor (lSM), face somatomotor (fSM), hand somatomotor (hSM), auditory (Aud), premotor (PMot), and cingulo-opercular (CON) networks. See Figure 1A for an example subject's networks.

Parcels acting as connector hubs were identified using the participation coefficient (PC) metric (Guimerà et al., 2007), a measure of how much a network node (here, a parcel) connects to multiple modules (brain networks). Across MSC subjects, the PC was highest in the lateral and ventromedial prefrontal and lateral and medial parietal cortex (Figure 1B). This distribution was replicated in HCP data (Figure S1A).

To focus only on the most interconnected regions, we defined connector hubs in each individual as parcels in the 80th+ percentile of the PC. Additional analyses using different thresholds revealed effectively identical results (Figure S1C). Parcels with a low degree (in the bottom 25th percentile) were excluded from consideration (following Bertolero et al., 2015) because weakly connected regions are unlikely to have strong integrative influences on brain networks (Guimerà et al., 2007). We then clustered hubs across subjects based on their connectivity strength to each network using an algorithm that optimized the number of clusters to maximize modularity, which ensures similar network connectivity within clusters and dissimilar connectivity between clusters.

This clustering revealed three discrete sets, or categories, of hubs (Figure 1C) that exhibited strong modularity (modularity value [Q] = 0.44). These connectivity profiles are illustrated in Figure 1D, the spatial distributions of these hub sets are shown in Figure 1E, and the distribution of network identities of each hub set can be seen in Figure S1D. The first set of hubs exhibited relatively strong connectivity with FPN, DMN, and CAN. We termed these hubs "control-default connector hubs," and they localized to the dorsal angular gyrus, superior and inferior frontal gyrus, retrosplenial cortex, precuneus, and ventromedial prefrontal cortex. The second set exhibited strong connectivity among CON, DAN, and FPN. We termed these hubs "cross-control connector hubs." They localized to the inferior parietal lobule, supramarginal gyrus, middle and superior frontal gyrus, and posterior precuneus. The third set exhibited strong connectivity with sensory and motor processing systems (lVis, Aud, PMot, and the somatomotor networks hSM, fSM, and lSM) as well as CON and DAN. We termed these hubs "control-processing connector hubs." They localized to the pre and postcentral gyrus, lateral occipital cortex, dorsomedial prefrontal cortex, and posterior insula. Analyses of HCP data produced clusters similar to the above hub sets in both connectivity profiles and spatial distributions (Figure S1B), suggesting that these hub categories generalize across subject populations.

Notably, detection of these hub categories required the use of individual-specific hubs. When we clustered hubs derived from group average data, hub sets were not consistent across MSC and HCP datasets in number of clusters or network connectivity patterns, and neither group average dataset produced hub clusters similar to the individual-level clusters (Figure S1E).

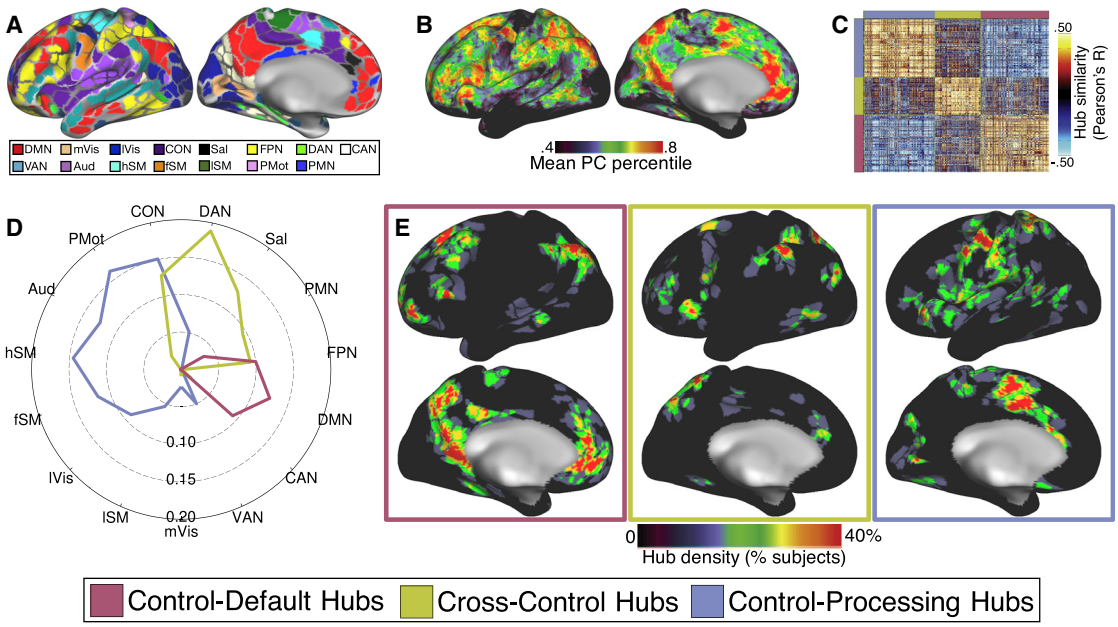

Figure 1. Hubs Cluster into Distinct Sets

(A) Network identities of cortical parcels in an example subject (MSC01).

(B) Spatial distributions of the participation coefficient (PC) percentile values across MSC subjects.

(C) A subject hub × subject hub matrix illustrating the similarity of network connectivity between hubs.

(D) Average network connectivity of each set of hubs. The line color indicates the hub set.

(E) Spatial distribution of hubs in each set. The border color indicates the hub set.

See the text for network abbreviations.

Figure 2 illustrates the network organization of connector hubs in one subject (MSC01) using spring embedding plots at a connection density of 1.5%, as implemented in Gephi (https://gephi.org/). See Figure S2 for plots of all MSC subjects. Figure 2A shows the locations and network identities of hubs on the cortex. The spring embedding plot below illustrates connectional relationships between networks and highlights the hubs. Figure 2B shows the same plots, with parcels colored by connector hub category. This visualization illustrates how hubs in the same category cluster together in network space; how hubs exist primarily at boundary points between different networks; how different hub categories mediate between different networks; and how hubs of the same category can have multiple network identities.

Removing Specific Sets of Hubs Separates Brain Networks in Distinct Ways

If hubs in different categories represent links between specific networks, then lesions to hubs in one category could isolate those networks from the brain's network structure. We artificially simulated hub category-specific lesions by removing all hubs in each category in turn and examining the effects on network structure (Albert et al., 2000; de Reus and van den Heuvel, 2014). These effects were quantified by calculating the average path length (a measure of how easily a node can connect to any other node) of all regions in each network after removal of the hub nodes, averaged across many density thresholds (from 0.3% to 5%). A greater path length indicates increasing network isolation. This measure was compared (using paired t tests) with path lengths calculated after removing the same number of randomly chosen, degree-matched non-hubs, averaged across 100 iterations. Here we report results for hSM, CON, FPN, and DMN networks; see Table S1 for results from all networks. Significance was Bonferroni-corrected for the number of hub sets × networks tested.

Figure 3 illustrates effects of removing hubs in each category from the network. Compared with the original network structure (Figure 3A), removing control-default connector hubs isolated the DMN in subject MSC01 (Figure 3B). Across MSC subjects, removing these hubs increased the path lengths for DMN and FPN (t-statistic [ts](9) > 7, p values [ps] < 0.01) but not CON or hSM (ps > 0.5; Figure 3C). Removal of cross-control connector hubs separated FPN and CON in MSC01 (Figure 3D) and, across subjects, increased the path lengths for FPN and CON (ts(9) > 4.4, ps < 0.05) but not hSM or DMN (ps > 0.05; Figure 3E). Removal of control-processing hubs isolated lVis and caused hSM, fSM, and Aud networks to break off of the network structure in MSC01 (Figure 3F). Across subjects, removing these hubs increased the path lengths for hSM and CON (ts(9) > 5.4, ps < 0.01) but not for FPN or DMN (ps > 0.2; Figure 3G). When only subsets of each hub category were removed, the same network-specific path lengths progressively increased relative to the proportion of removed hubs (Figure S3A). Similar effects were observed in the HCP dataset (Figure S3B). These findings suggest that damage to different hub categories has dissociable effects on the brain's network organization.

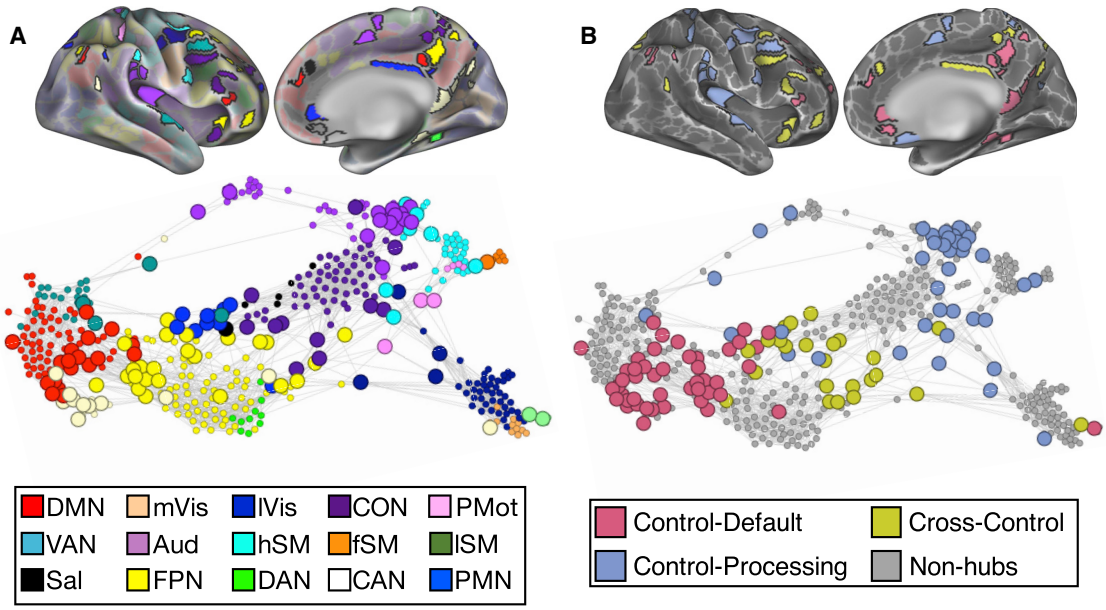

Figure 2. Organization of Networks and Hub Sets in a Single Subject

(A) Network identities of cortical parcels in a single subject (top) and a spring embedding plot (bottom), illustrating relationships between these parcels. Hubs are highlighted on the cortex and enlarged in the spring embedding plot.

(B) The same parcels and plot, with parcels colored based on the hub set.

See the text for network abbreviations.

Task Activations Are Influenced by Hub Category and Network Identity

Different RSFC-derived brain networks are considered discrete sets of brain regions, in part because they are differentially engaged during performance of cognitive and motor tasks (Smith et al., 2009). If the hub categories identified here are also discrete sets of brain regions, then they similarly may exhibit category-specific responses during task performance that can be dissociable from the behavior of their containing network. To test this question, we examined whether the category of a hub region explains variance in task activation beyond that explained by brain network identity.

For each subject, we calculated the average task activation within each hub parcel for multiple task contrasts. The MSC data include a motor task, a mixed task (including spatial coherence discrimination and verbal discrimination conditions), and an implicit memory task. For each task, we entered activations of all hub regions into an ANOVA, testing for effects of network identity and hub category while controlling for subject identity. Significance was Bonferroni-corrected for the number of tasks tested. Contrasts against baseline (prestimulus baseline for event-related designs and implicit baseline for blocked designs) were used to obtain the most complete picture of brain activation. Here we present findings from activation patterns averaged across all conditions in each task, but tests of condition-specific effects produced similar results (Figures S4A–S4D).

We found that network identity was a highly significant factor explaining variance in all task activations (F statistics [Fs](16,1211) > 7.5, ps << 0.001). Critically, hub category was also a highly significant explanatory factor (Fs(2,1211) > 44.0, ps << 0.001). Further, the variance in activation explained by hub category was comparable with that explained by network identity in the motor (hub type, 4%; network, 5%) and mixed (hub type, 6%; network, 8%) tasks (but was lower in the implicit memory task: hub type, 4%; network, 19%) (Figure 4A).

We examined details of these hub category effects by plotting residual activations after controlling for subject and network identity (Figure 4B). We observed that control-default hubs deactivated in all tasks. By contrast, control-processing hubs activated during all tasks, whereas cross-control hubs activated during the mixed and implicit memory tasks but not the motor task. Because network identity was controlled, the deactivation of control-default hubs cannot be attributed to known DMN deactivations but represent deactivations above and beyond network-level effects. Specifically, control-default hubs in DMN deactivated more across tasks than DMN non-hubs (Figure S4I).

The function of connector hubs within control networks is of particular interest in the performance of cognitive tasks (Cole et al., 2013; Gratton et al., 2018). To investigate the effect of hub category on activation within control networks, we repeated the above ANOVAs, restricting analysis to hubs in the FPN, CON, and DAN.

For FPN/CON/DAN hubs, network identity did *not* significantly explain task activation in the motor or the mixed task (<1.5% variance, Fs(2,472) < 5.0, ps > 0.1) (Figure 4C). This indicates that control networks cannot be distinguished from each other based on their activations in these two tasks. In the implicit memory task, network identity did explain task activation (6.0% variance,

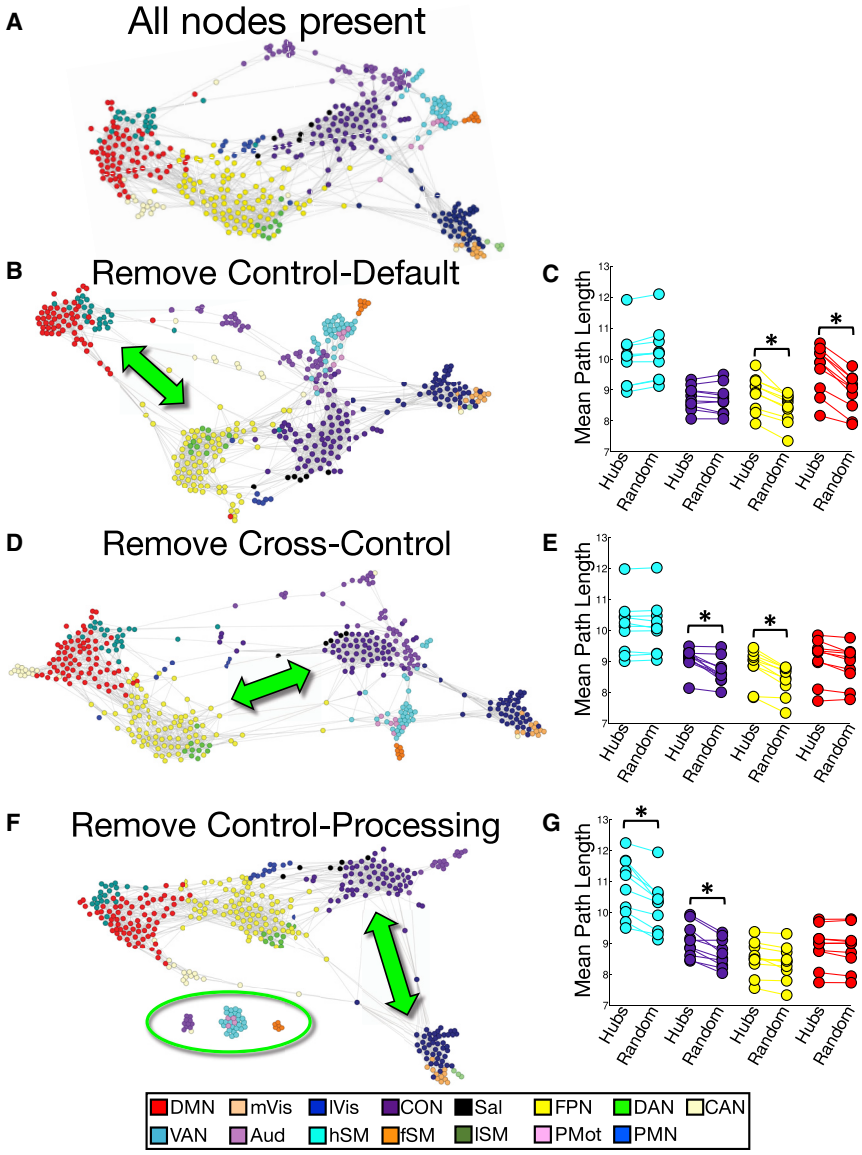

Figure 3. Removing Hubs Alters Network Structure Depending on the Hub Category Removed

(A) The network structure of a single subject.

(B, D, and F) Network structures after removing control-default (B), cross-control (D), and control-processing (F) hub nodes. Arrows indicate network structure changes; the circle indicates isolated networks.

(C, E, and G) Average path lengths for each network after removing control-default (C), cross-control (E), or control-processing (G) hubs (x axes, hubs) compared with removal of random, degree-matched non-hubs (x axes, random).

Effects are shown for hSM (cyan), CON (purple), FPN (yellow), and DMN (red). *, significant difference from random removal.

F(2,472) = 20.2, p << 0.001). By contrast, hub category was a significant explanatory factor across all tasks (Fs(2,472) > 50, ps << 0.001) and explained more variance in activation than network identity in all tasks (motor, 9.7%; mixed, 15.9%; implicit memory, 15.6%). Examination of these hub category effects (Figure 4D) revealed a similar pattern as that observed using all hubs (Figure 4B). Notably, we observed task deactivations in control-default hubs even when restricting analysis to canonically "task-positive" networks. For example, although FPN non-hubs showed the expected task-positive activations, FPN control-default hubs actually deactivated across tasks (Figure S4I). Together, these findings suggest that, within control networks, a hub's category can be as or more important for understanding its function than the hub's network identity. These effects of hub category on task activation were broadly replicated in the HCP data (Figures S4E–S4H), although hub category explained less variance in this dataset, possibly because of less per-individual task data (≤5 min/task), resulting in noisier activations.

DISCUSSION

Connector hubs are considered brain regions of high importance because of their proposed role of enabling interactions between control and processing systems (Mesulam, 1990), allowing flexible control of cognition and behavior (Bertolero et al., 2017; Gratton et al., 2018; Power et al., 2013). Investigating the function of hubs and the potential effect of damage to hubs is thus of great neuroscientific interest. Investigations of this type have revealed broad principles about how hubs are engaged during task performance (Bertolero et al., 2015; Chan et al., 2017; Cohen and D'Esposito, 2016; Cole et al., 2013; Gratton et al., 2016; Hwang et al., 2017; Mattar et al., 2015; Shine et al., 2016), how they are affected by aging (Chan et al., 2017; Spreng and Schacter, 2012), and how lesions to hubs affect cognition (Warren et al., 2014). However, the effect of such investigations may be limited by the treatment of hubs as belonging to a single category. By contrast, the present findings demonstrate the existence of three discrete sets of connector hubs, each with a disparate pattern of network connections and task-evoked responses.

Critically, determinations of hub category must be made at the level of the individual. Brain networks are spatially variable across individuals (Gordon et al., 2017), and the present work demonstrates both inter-individual variability in the locations of hubs (Figure 1) and that hubs in different categories can be spatially adjacent within an individual (Figure 2B). Likely as a result, these hub categories could not be identified using group average data (Figure S1E). This illustrates the need for individual specificity in hub identification.

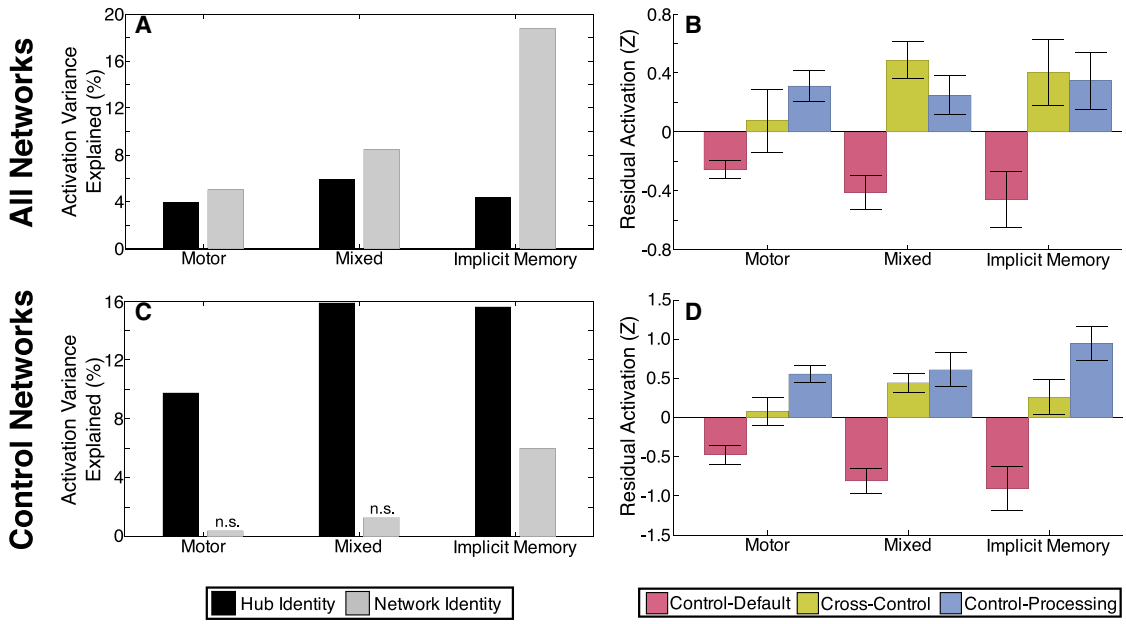

Figure 4. Hub Category Explains Significant Variance in Task Activations, Especially within Control Networks

(A and C) Variance in task activation in the MSC dataset explained by hub category and network identity, in all hubs (A) and in CON/FP/DAN hubs (C). Effects were significant except where noted (not significant, n.s.).

(B and D) Residual task activations (after controlling for subject and network identity) for each hub category, in all hubs (B) and in CON/FPN/DAN hubs (D). Error bars represent SD across subjects.

Different Hub Categories Integrate Different Aspects of Human Brain Function

Clustering hubs by their network connections revealed three discrete categories of connector hubs. The separability of these hub categories is supported by the relatively high modularity of the clustering ($Q > 0.4$), the replication of clusters in the independent HCP dataset, the varying effects on the brain's network structure after removing each category of hubs, and the different task-evoked responses observed in different hub categories.

All three sets of hubs were linked to at least one control network (FPN, CON, or DAN). This finding converges with work by Cole et al. (2012, 2013), Mattar et al. (2015), and Shine et al. (2016), arguing for high integrative function in control regions during complex tasks, and it refines the concept advanced by Gratton et al. (2018) that connector hubs allow control networks to interact with processing networks to enable goal-directed cognition. Indeed, we propose that, by integrating information between specific sets of control and processing brain systems, these three hub categories may each be important for specific control behaviors. First, a set of control-default connector hubs linked the DMN and FPN. These hubs may allow regulation of internally generated processes associated with the DMN, such as memories, emotional responses, or planning (Andrews-Hanna et al., 2014; Dixon et al., 2018; Spreng and Schacter, 2012), and disruption of these hubs may be linked to the altered connectivity between DMN and control systems observed in disorders of emotional regulation (Kaiser et al., 2015). Second, a set of control-processing hubs linked sensory and motor systems to the CON and DAN. Among other functions, these hubs may enable goal-directed control of motor function (Rinne et al., 2018), potentially enabling the changes in network integration observed during motor task automatization (Mohr et al., 2016). Third, a set of cross-control hubs linked control networks to each other. During complex cognitive tasks, these hubs may integrate control networks to enable recursive "control of control" operations in which one network exhibits sustained control to regulate the dynamic top-down control functions of another network (Braver and Cohen, 2000; Cohen et al., 2014; Dosenbach et al., 2008; Gratton et al., 2016; Vatansever et al., 2015).

Together, these results argue against connector hubs forming a unified network core that regulates peripheral processing systems. Instead, they suggest a model of brain organization in which connector hubs enable separate top-down control of multiple parallel processing streams representing internal and external stimuli as well as allowing high-level integration of those control functions.

Task-Evoked Activity Is Driven in Opposing Directions by Different Hub Categories

These interpretations of hub category functions are supported by observed differences in task-evoked activity. Control-default hubs were deactivated by all tasks, whereas control-processing hubs were active during all tasks, and cross-control hubs were only active during tasks requiring configuring of input, transformation, and output processes.

Across all hubs, both hub category and network identity explained independent variance in task activation. However, among control networks, a hub's category explained task activation better than its network membership across all MSC and some HCP tasks. Indeed, for some task contrasts in both

datasets, activation did not differ between control networks. Although functional differences between control networks are well established (Dosenbach et al., 2006, 2007, 2008), the common coactivation among these networks means that, under many task conditions, the networks cannot be easily distinguished (Fedorenko et al., 2013), particularly when task initiation and/or maintenance signals are not assessed. However, control network hubs of different categories were distinguishable, even under task conditions where network-level functions could not be dissociated. This suggests that hub functions are influenced not only by their network membership but also by their specific integrative links within the network structure. Hub category thus appears to be an additional organizational principle that influences brain function independently of network membership.

Implications for Lesion and Brain Stimulation Studies

Recent lesion work has focused on how localized damage may affect the function of connected regions (Gratton et al., 2012) and so influence behavioral impairment (He et al., 2007; Siegel et al., 2016) or recovery (He et al., 2007; Siegel et al., 2018). Damage to hubs may have widespread effects on brain networks (Gratton et al., 2012), causing dramatic behavioral impairment (Warren et al., 2014). The present dissociation of hubs into multiple categories and the observation that simulated damage to a hub category isolates specific networks (Figure 3) allows the formulation of specific hypotheses about which behaviors may be affected by lesions to which hubs—e.g., that damage to cross-control hubs may affect task switching but not automatic sensory motor functions.

Hubs may also represent ideal targets for stimulation using TMS because induced modification of hub activity could influence multiple networks and, thus, have increased experimental or clinical effects (Lynch et al., 2018). The present work enables predictions about which behaviors may be influenced by targeting which hub regions. For example, protocols for treatment of depression using prefrontally targeted TMS could potentially be improved by specific targeting of a patient's control-default hubs, thus enhancing FPN regulation of DMN-related emotional circuits. Such possibilities remain to be investigated in future work.

Potential Alternate Accounts of Hub Function

Prior work has suggested that control regions regulate the function of processing regions (Miller and D'Esposito, 2005; Zanto et al., 2011). Because the hub regions identified here are well positioned to enable information transfer between control and processing systems, we argue that control signal transmission is a likely function of these hubs (Gratton et al., 2018). However, there are other potential explanations for this observed topology. Control signals may be transmitted by some other, unknown means, and the hubs described here may instead compare control signals with the outputs of the influenced network to implement error-related adjustments. Or hub regions may be "domain-general" regions that are multiply connected at rest because they can be dynamically recruited to assist with the functions of multiple brain systems. Although we consider such alternative accounts unlikely—the hub categories' spatial distributions do not correspond with either known error signals (e.g., Neta et al., 2015) or putative domain-general regions (Fedorenko et al., 2013)—they should be tested in future work using task paradigms designed to dissociate such possibilities.

STAR★METHODS

Detailed methods are provided in the online version of this paper and include the following:

- KEY RESOURCES TABLE
- CONTACT FOR REAGENT AND RESOURCE SHARING
- EXPERIMENTAL MODEL AND SUBJECT DETAILS
  - Midnight Scan Club (MSC) dataset
  - Human Connectome Project (HCP) Dataset
- METHOD DETAILS
  - Midnight Scan Club (MSC) dataset
  - Human Connectome Project (HCP) Dataset
- QUANTIFICATION AND STATISTICAL ANALYSIS
  - Parcellation
  - Hub identification
  - Hub clustering
  - Effects of hub type removal on brain network structure
  - Effect of hub type on task activation
- DATA AND SOFTWARE AVAILABILITY

SUPPLEMENTAL INFORMATION

Supplemental Information includes four figures and one table and can be found with this article online at https://doi.org/10.1016/j.celrep.2018.07.050.

ACKNOWLEDGMENTS

This work was supported by NIH grants NS088590 and TR000448 (to N.U.F.D.) and MH104592 (to D.J.G.); the Jacobs Foundation (to N.U.F.D.); the Child Neurology Foundation (to N.U.F.D.); the McDonnell Center for Systems Neuroscience (to N.U.F.D. and B.L.S.); the Mallinckrodt Institute of Radiology (to N.U.F.D.); the Hope Center for Neurological Disorders (to N.U.F.D., B.L.S., and S.E.P.); an American Psychological Association dissertation research award (to A.W.G.); and the McDonnell Foundation (to S.E.P.). The views expressed in this article are those of the authors and do not necessarily reflect the position or policy of the Department of Veterans Affairs or the United States government.

AUTHOR CONTRIBUTIONS

A.W.G., A.L.N., D.J.G., S.M.N., and N.U.F.D. collected the data. E.M.G., C.J.L., T.O.L., A.W.G., D.J.G., M.O., A.L.N., and C.G. processed and analyzed the data. E.M.G., C.J.L., C.G., D.J.G., B.L.S., S.E.P., N.U.F.D., and S.M.N. wrote the paper with input from all authors.

DECLARATION OF INTERESTS

The authors declare no competing interests.

Received: March 8, 2018
Revised: May 31, 2018
Accepted: July 16, 2018
Published: August 14, 2018

REFERENCES

Albert, R., Jeong, H., and Barabási, A.-L. (2000). Error and attack tolerance of complex networks. Nature *406*, 378–382.

Andrews-Hanna, J.R., Smallwood, J., and Spreng, R.N. (2014). The default network and self-generated thought: component processes, dynamic control, and clinical relevance. Ann. N Y Acad. Sci. *1316*, 29–52.

Bertolero, M.A., Yeo, B.T.T., and D'Esposito, M. (2015). The modular and integrative functional architecture of the human brain. Proc. Natl. Acad. Sci. USA *112*, E6798–E6807.

Bertolero, M.A., Yeo, B.T.T., and D'Esposito, M. (2017). The diverse club. Nat. Commun. *8*, 1277.

Braver, T., and Cohen, J. (2000). On the Control of Control: The Role of Dopamine in Regulating Prefrontal Function and Working Memory. In Attention and Performance XVIII: Control of Cognitive Processes, S. Monsell and J. Driver, eds. (Cambridge, MA: MIT Press), 713–737.

Chan, M.Y., Alhazmi, F.H., Park, D.C., Savalia, N.K., and Wig, G.S. (2017). Resting-State Network Topology Differentiates Task Signals across the Adult Life Span. J. Neurosci. *37*, 2734–2745.

Cohen, J.R., and D'Esposito, M. (2016). The Segregation and Integration of Distinct Brain Networks and Their Relationship to Cognition. J. Neurosci. *36*, 12083–12094.

Cohen, J.R., Gallen, C.L., Jacobs, E.G., Lee, T.G., and D'Esposito, M. (2014). Quantifying the reconfiguration of intrinsic networks during working memory. PLoS ONE *9*, e106636.

Cole, M.W., Yarkoni, T., Repovš, G., Anticevic, A., and Braver, T.S. (2012). Global connectivity of prefrontal cortex predicts cognitive control and intelligence. J. Neurosci. *32*, 8988–8999.

Cole, M.W., Reynolds, J.R., Power, J.D., Repovs, G., Anticevic, A., and Braver, T.S. (2013). Multi-task connectivity reveals flexible hubs for adaptive task control. Nat. Neurosci. *16*, 1348–1355.

Dale, A.M., Fischl, B., and Sereno, M.I. (1999). Cortical surface-based analysis. I. Segmentation and surface reconstruction. Neuroimage *9*, 179–194.

de Reus, M.A., and van den Heuvel, M.P. (2014). Simulated rich club lesioning in brain networks: a scaffold for communication and integration? Front. Hum. Neurosci. *8*, 647.

Dixon, M.L., Vega, A.D.L., Mills, C., Andrews-Hanna, J., Spreng, R.N., Cole, M.W., and Christoff, K. (2018). Heterogeneity within the frontoparietal control network and its relationship to the default and dorsal attention networks.*115* (Proc. Natl. Acad. Sci.), E1598–E1607.

Dosenbach, N.U.F., Visscher, K.M., Palmer, E.D., Miezin, F.M., Wenger, K.K., Kang, H.C., Burgund, E.D., Grimes, A.L., Schlaggar, B.L., and Petersen, S.E. (2006). A core system for the implementation of task sets. Neuron *50*, 799–812.

Dosenbach, N.U.F., Fair, D.A., Miezin, F.M., Cohen, A.L., Wenger, K.K., Dosenbach, R.A.T., Fox, M.D., Snyder, A.Z., Vincent, J.L., Raichle, M.E., et al. (2007). Distinct brain networks for adaptive and stable task control in humans. Proc. Natl. Acad. Sci. USA *104*, 11073–11078.

Dosenbach, N.U.F., Fair, D.A., Cohen, A.L., Schlaggar, B.L., and Petersen, S.E. (2008). A dual-networks architecture of top-down control. Trends Cogn. Sci. *12*, 99–105.

Duncan, J., and Owen, A.M. (2000). Common regions of the human frontal lobe recruited by diverse cognitive demands. Trends Neurosci. *23*, 475–483.

Fedorenko, E., Duncan, J., and Kanwisher, N. (2013). Broad domain generality in focal regions of frontal and parietal cortex. Proc. Natl. Acad. Sci. USA *110*, 16616–16621.

Glasser, M.F., Sotiropoulos, S.N., Wilson, J.A., Coalson, T.S., Fischl, B., Andersson, J.L., Xu, J., Jbabdi, S., Webster, M., Polimeni, J.R., et al.; WU-Minn HCP Consortium (2013). The minimal preprocessing pipelines for the Human Connectome Project. Neuroimage *80*, 105–124.

Gordon, E.M., Laumann, T.O., Adeyemo, B., Huckins, J.F., Kelley, W.M., and Petersen, S.E. (2016). Generation and Evaluation of a Cortical Area Parcellation from Resting-State Correlations. Cereb. Cortex *26*, 288–303.

Gordon, E.M., Laumann, T.O., Gilmore, A.W., Newbold, D.J., Greene, D.J., Berg, J.J., Ortega, M., Hoyt-Drazen, C., Gratton, C., Sun, H., et al. (2017). Precision Functional Mapping of Individual Human Brains. Neuron *95*, 791–807.e7.

Gratton, C., Nomura, E.M., Pérez, F., and D'Esposito, M. (2012). Focal brain lesions to critical locations cause widespread disruption of the modular organization of the brain. J. Cogn. Neurosci. *24*, 1275–1285.

Gratton, C., Laumann, T.O., Gordon, E.M., Adeyemo, B., and Petersen, S.E. (2016). Evidence for Two Independent Factors that Modify Brain Networks to Meet Task Goals. Cell Rep. *17*, 1276–1288.

Gratton, C., Sun, H., and Petersen, S.E. (2018). Control networks and hubs. Psychophysiology *55*, e13032.

Guimerà, R., Sales-Pardo, M., and Amaral, L.A.N. (2007). Classes of complex networks defined by role-to-role connectivity profiles. Nat. Phys. *3*, 63–69.

He, B.J., Snyder, A.Z., Vincent, J.L., Epstein, A., Shulman, G.L., and Corbetta, M. (2007). Breakdown of functional connectivity in frontoparietal networks underlies behavioral deficits in spatial neglect. Neuron *53*, 905–918.

Hwang, K., Bertolero, M.A., Liu, W.B., and D'Esposito, M. (2017). The Human Thalamus Is an Integrative Hub for Functional Brain Networks. J. Neurosci. *37*, 5594–5607.

Kaiser, R.H., Andrews-Hanna, J.R., Wager, T.D., and Pizzagalli, D.A. (2015). Large-Scale Network Dysfunction in Major Depressive Disorder: A Meta-analysis of Resting-State Functional Connectivity. JAMA Psychiatry *72*, 603–611.

Lancichinetti, A., and Fortunato, S. (2012). Consensus clustering in complex networks. Sci. Rep. *2*, 336.

Lynch, C.J., Breeden, A.L., Gordon, E.M., Cherry, J.B.C., Turkeltaub, P.E., and Vaidya, C.J. (2018). Precision inhibitory stimulation of individual-specific cortical hubs slows information processing in humans. bioRxiv. https://doi.org/10.1101/254417.

Marcus, D., Harwell, J., Olsen, T., Hodge, M., Glasser, M., Prior, F., Jenkinson, M., Laumann, T., Curtiss, S., and Van Essen, D. (2011). Informatics and Data Mining Tools and Strategies for the Human Connectome Project. Front. Neuroinform, Published online June 27, 2011. https://doi.org/10.3389/fninf.2011.00004.

Mattar, M.G., Cole, M.W., Thompson-Schill, S.L., and Bassett, D.S. (2015). A Functional Cartography of Cognitive Systems. PLoS Comput. Biol. *11*, e1004533.

Mesulam, M.M. (1990). Large-scale neurocognitive networks and distributed processing for attention, language, and memory. Ann. Neurol. *28*, 597–613.

Mesulam, M.M. (1998). From sensation to cognition. Brain *121*, 1013–1052.

Miezin, F.M., Maccotta, L., Ollinger, J.M., Petersen, S.E., and Buckner, R.L. (2000). Characterizing the hemodynamic response: effects of presentation rate, sampling procedure, and the possibility of ordering brain activity based on relative timing. Neuroimage *11*, 735–759.

Miller, B.T., and D'Esposito, M. (2005). Searching for "the top" in top-down control. Neuron *48*, 535–538.

Mohr, H., Wolfensteller, U., Betzel, R.F., Mišić, B., Sporns, O., Richiardi, J., and Ruge, H. (2016). Integration and segregation of large-scale brain networks during short-term task automatization. Nat. Commun. *7*, 13217.

Neta, M., Miezin, F.M., Nelson, S.M., Dubis, J.W., Dosenbach, N.U.F., Schlaggar, B.L., and Petersen, S.E. (2015). Spatial and temporal characteristics of error-related activity in the human brain. J. Neurosci. *35*, 253–266.

Posner, M.I., and Petersen, S.E. (1990). The attention system of the human brain. Annu. Rev. Neurosci. *13*, 25–42.

Power, J.D., and Petersen, S.E. (2013). Control-related systems in the human brain. Curr. Opin. Neurobiol. *23*, 223–228.

Power, J.D., Cohen, A.L., Nelson, S.M., Wig, G.S., Barnes, K.A., Church, J.A., Vogel, A.C., Laumann, T.O., Miezin, F.M., Schlaggar, B.L., and Petersen, S.E. (2011). Functional network organization of the human brain. Neuron *72*, 665–678.

Power, J.D., Schlaggar, B.L., Lessov-Schlaggar, C.N., and Petersen, S.E. (2013). Evidence for hubs in human functional brain networks. Neuron *79*, 798–813.

Rinne, P., Hassan, M., Fernandes, C., Han, E., Hennessy, E., Waldman, A., Sharma, P., Soto, D., Leech, R., Malhotra, P.A., and Bentley, P. (2018). Motor

dexterity and strength depend upon integrity of the attention-control system. Proc. Natl. Acad. Sci. USA *115*, E536–E545.

Rosvall, M., and Bergstrom, C.T. (2008). Maps of random walks on complex networks reveal community structure. Proc. Natl. Acad. Sci. USA *105*, 1118–1123.

Rubinov, M., and Sporns, O. (2010). Complex network measures of brain connectivity: uses and interpretations. Neuroimage *52*, 1059–1069.

Shine, J.M., Bissett, P.G., Bell, P.T., Koyejo, O., Balsters, J.H., Gorgolewski, K.J., Moodie, C.A., and Poldrack, R.A. (2016). The Dynamics of Functional Brain Networks: Integrated Network States during Cognitive Task Performance. Neuron *92*, 544–554.

Siegel, J.S., Ramsey, L.E., Snyder, A.Z., Metcalf, N.V., Chacko, R.V., Weinberger, K., Baldassarre, A., Hacker, C.D., Shulman, G.L., and Corbetta, M. (2016). Disruptions of network connectivity predict impairment in multiple behavioral domains after stroke. Proc. Natl. Acad. Sci. USA *113*, E4367–E4376.

Siegel, J.S., Seitzman, B.A., Ramsey, L.E., Ortega, M., Gordon, E.M., Dosenbach, N.U.F., Petersen, S.E., Shulman, G.L., and Corbetta, M. (2018). Re-emergence of modular brain networks in stroke recovery. Cortex *101*, 44–59.

Smith, S.M., Jenkinson, M., Woolrich, M.W., Beckmann, C.F., Behrens, T.E.J., Johansen-Berg, H., Bannister, P.R., De Luca, M., Drobnjak, I., Flitney, D.E., et al. (2004). Advances in functional and structural MR image analysis and implementation as FSL. Neuroimage *23* (*Suppl 1*), S208–S219.

Smith, S.M., Fox, P.T., Miller, K.L., Glahn, D.C., Fox, P.M., Mackay, C.E., Filippini, N., Watkins, K.E., Toro, R., Laird, A.R., and Beckmann, C.F. (2009). Correspondence of the brain's functional architecture during activation and rest. Proc. Natl. Acad. Sci. USA *106*, 13040–13045.

Spreng, R.N., and Schacter, D.L. (2012). Default network modulation and large-scale network interactivity in healthy young and old adults. Cereb. Cortex *22*, 2610–2621.

van den Heuvel, M.P., and Sporns, O. (2013). Network hubs in the human brain. Trends Cogn. Sci. *17*, 683–696.

Van Essen, D.C., Ugurbil, K., Auerbach, E., Barch, D., Behrens, T.E.J., Bucholz, R., Chang, A., Chen, L., Corbetta, M., Curtiss, S.W., et al.; WU-Minn HCP Consortium (2012). The Human Connectome Project: a data acquisition perspective. Neuroimage *62*, 2222–2231.

Van Essen, D.C., Smith, S.M., Barch, D.M., Behrens, T.E., Yacoub, E., and Ugurbil, K.; WU-Minn Human Connectome Project: an overview. Neuroimage *80*, 62–79.

Vatansever, D., Menon, D.K., Manktelow, A.E., Sahakian, B.J., and Stamatakis, E.A. (2015). Default Mode Dynamics for Global Functional Integration. J. Neurosci. *35*, 15254–15262.

Warren, D.E., Power, J.D., Bruss, J., Denburg, N.L., Waldron, E.J., Sun, H., Petersen, S.E., and Tranel, D. (2014). Network measures predict neuropsychological outcome after brain injury. Proc. Natl. Acad. Sci. USA *111*, 14247–14252.

Yeo, B.T.T., Krienen, F.M., Sepulcre, J., Sabuncu, M.R., Lashkari, D., Hollinshead, M., Roffman, J.L., Smoller, J.W., Zöllei, L., Polimeni, J.R., et al. (2011). The organization of the human cerebral cortex estimated by intrinsic functional connectivity. J. Neurophysiol. *106*, 1125–1165.

Zanto, T.P., Rubens, M.T., Thangavel, A., and Gazzaley, A. (2011). Causal role of the prefrontal cortex in top-down modulation of visual processing and working memory. Nat. Neurosci. *14*, 656–661.

STAR★METHODS

KEY RESOURCES TABLE

REAGENT or RESOURCE	SOURCE	IDENTIFIER
Deposited Data		
MSC raw and processed MRI data	Gordon et al., 2017	https://openneuro.org/datasets/ds000224/versions/00002; Openneuro: ds000224
HCP raw and processed MRI data	Van Essen et al., 2013	https://www.humanconnectome.org/study/hcp-young-adult
Software and Algorithms		
MATLAB	Mathworks	RRID:SCR_001622 https://www.mathworks.com/
Connectome Workbench	Marcus et al., 2011	RRID:SCR_008750 https://www.humanconnectome.org/software/connectome-workbench.html
Freesurfer	Dale et al., 1999	RRID:SCR_001847 https://surfer.nmr.mgh.harvard.edu/
FSL	Smith et al., 2004	RRID:SCR_002823 https://fsl.fmrib.ox.ac.uk/fsl/fslwiki
4dfp tools		ftp://imaging.wustl.edu/pub/raichlab/4dfp_tools/
Freesurfer to fs_LR pipeline	Van Essen et al., 2012	http://brainvis.wustl.edu/index.html/
Parcellation code	Gordon et al., 2016	https://sites.wustl.edu/petersenschlaggarlab/files/2018/06/Gordon2016Surface_parcellation_distribute-20agwt4.zip
Brain connectivity toolbox	Rubinov and Sporns, 2010	RRID:SCR_004841 http://sites.google.com/site/bctnet/
Infomap	Rosvall and Bergstrom, 2008	http://www.mapequation.org

CONTACT FOR REAGENT AND RESOURCE SHARING

Further information and requests for resources should be directed to and will be fulfilled by the Lead Contact, Dr. Evan M. Gordon (evan.gordon@va.gov).

EXPERIMENTAL MODEL AND SUBJECT DETAILS

Data was used from two independent publicly available datasets of fMRI data, described below.

Midnight Scan Club (MSC) dataset

Data were collected from ten healthy, right-handed, young adult subjects (5 females; age: 24-34). Two of the subjects are authors (NUFD and SMN), and the remaining subjects were recruited from the Washington University community. Informed consent was obtained from all participants. The study was approved by the Washington University School of Medicine Human Studies Committee and Institutional Review Board. This dataset was previously reported in (Gordon et al., 2017).

Human Connectome Project (HCP) Dataset

Resting-state and task data from 80 subjects (40 females; mean age = 29 years, age range = 22-36) were retrieved from the publicly available Human Connectome Project (HCP) dataset (Van Essen et al., 2012). These subjects were selected as the subjects with minimal in-scan resting-state head motion estimates from the S500 data release.

METHOD DETAILS

Midnight Scan Club (MSC) dataset

Imaging for each subject was performed on a Siemens TRIO 3T MRI scanner over the course of 12 sessions conducted on separate days, each beginning at midnight. In total, four T1-weighted images, 5 hours of resting-state BOLD fMRI, and 5.5 hours of task BOLD fMRI were collected from each subject. Tasks collected included a motor task, a mixed perceptual/language task, and an implicit memory task. Data was processed and normalized into CIFTI space using tools from the Freesurfer (Dale et al., 1999), FSL (Smith et al., 2004), and Connectome Workbench (Marcus et al., 2011) software packages, as in (Gordon et al., 2017). Task evoked activations were modeled individually for each voxel with a general linear model (GLM) (Miezin et al., 2000), using in-house image analysis

software written in IDL (Research Systems, Inc.). For further details, including data acquisition parameters and preprocessing steps, see (Gordon et al., 2017).

Human Connectome Project (HCP) Dataset

See (Van Essen et al., 2012) for details of the data acquisition procedures. Briefly, structural and functional MRI data were acquired on a custom Siemens Skyra 3T scanner, including one T1-weighted image and four 15-minute resting-state BOLD runs. The two runs (one each of left-right/right-left phase-encoding) with minimal in-scan motion were selected for each subject.

Functional images were processed using the HCP minimal preprocessing pipeline (Glasser et al., 2013), which includes head motion correction, intensity normalization, bias field correction, and transformation to an isotropic 2-mm MNI atlas space. Volumetric data was then processed into CIFTI space as in as in (Gordon et al., 2017).

Pre-computed CIFTI-space task contrasts for each subject were retrieved from the HCP dataset for each of the seven separate tasks in the dataset (Emotion, Gambling, Language, Motor, Relational, Social, and Working Memory).

QUANTIFICATION AND STATISTICAL ANALYSIS

Parcellation

Each subject's cortex was parcellated into discrete homogeneous parcels using a gradient-based parcellation technique (Gordon et al., 2016). Briefly, for each subject, RSFC time courses from all points in the brain were correlated against each other to generate a correlation map seeded from every point, and then these maps were correlated against each other to calculate the similarity of RSFC maps between each pair of points in the brain. A map of spatial gradients was then calculated on each column of the resulting similarity matrix using Workbench tools. Edges were identified in each of the resulting gradient maps using the watershed edge detection technique (S. Beucher and C. Lantuejoul, 1979, International Workshop on Image Processing: Real-Time Edge and Motion Detection/Estimation, conference), and all resulting edge maps were summed. Parcels were built from the resulting summed edge map by again applying the watershed edge detection technique. Neighboring parcels with edge counts less than a predefined threshold were merged. This threshold was varied across datasets based on the observed level of noise in the data. The threshold was set at the 50^{th} %tile of all edge values for the MSC subjects and at the 70^{th} %tile for the HCP subjects.

Hub identification

In each subject, parcels acting as hubs were identified using the participation coefficient (PC) metric, a measure of the degree to which a node in a graph (here, a parcel) is connected to multiple separate modules (here, brain networks). First, the subject's RSFC time courses were averaged across the vertices of each parcel to create parcel average time courses. These parcel average time courses were then cross-correlated against each other to create a parcel-to-parcel correlation matrix, which was then Fisher-transformed to improve normality. Correlations between parcels with centroids within 30mm geodesic distance of each other were set to zero in the matrix. The matrix was thresholded at a range of graph densities ranging from 0.3% to 5%, and the Infomap algorithm (Rosvall and Bergstrom, 2008) was applied to each thresholded matrix in order to identify communities. At each density threshold, these infomap-derived communities were used to calculate PC for each parcel, as in (Guimerà et al., 2007). Because the PC calculation uses parcel degree in the denominator, parcels with low degree can produce unstable (and often large) PC values, even though a parcel with low degree is unlikely to be a hub of interest. Thus, the PC values for parcels with degree in the bottom 25^{th} percentile of all parcels were set to zero. PC values were then converted to percentiles and averaged across density thresholds.

There is currently no accepted cutoff for what constitutes a hub versus a non-hub. As a result, we defined hubs as parcels with PC values in the top Xth percentile within each subject (following (Bertolero et al., 2015; Gratton et al., 2016), where X ranges from 75 to 95. Here, we present results using the top 80^{th} percentile PC value parcels as hubs; however, we note that effectively identical results were obtained for all PC cutoffs tested (Figure S1C).

Hub clustering

We observed that high-PC hub parcels varied in their connectivity profiles. We tested whether hubs could be clustered into discrete types across individuals. For each subject, we first identified individual-specific large-scale cortical networks. The infomap-derived communities identified at each density threshold (above) were assigned network identities based on similarities to known group-average networks [e.g., the seventeen networks described in (Gordon et al., 2017); see Figure S1B]. This matching approach proceeded following (Gordon et al., 2017). At each density threshold, all identified communities within an individual were compared (using spatial overlap, quantified with the Jaccard index) to each one of the group-average networks in turn. The best-matching (highest-overlap) community was assigned that network identity; that community was not considered for comparison with other networks within that threshold. Matches lower than Jaccard = 0.1 were not considered (to avoid matching based on only a few vertices). Matches were first made with the large, well-known networks (Default, Lateral Visual, Motor, Cingulo-Opercular, Fronto-Parietal, Dorsal Attention), and then to the smaller, less well-known networks (Ventral Attention, Salience, Parietal Memory, Contextual Association, Medial Visual, Motor Foot). In each individual, a final "consensus" network assignment was then derived by collapsing assignments across thresholds, giving each node the assignment it had at the sparsest possible threshold at which it was successfully assigned to one of the known group networks.

We then calculated the strength of functional connectivity between the hub parcel and all parcels of each network, averaged across all within-network parcels outside of 30mm from the hub. This resulted in a network connectivity profile (i.e., 17 independent connectivity strengths) for each hub.

Discrete hub types were identified by clustering together similar network connectivity profiles. Similarity of network connectivity profiles was calculated by cross-correlating the network profiles of all subject hubs, separately in each dataset. The Louvain algorithm was applied to the resultant weighted, signed correlation matrix 10^3 times, and a separate consensus clustering was generated using an "association-recluster" strategy, which addresses the issue that modularity-based clusterings are often non-deterministic. In an association-recluster framework, modularity maximization is used to create a consensus clustering from an association matrix, where entries denote the frequency with which nodes co-occur in a community across iterations (Lancichinetti and Fortunato, 2012).

Finally, hub detection and clustering were repeated on "group average" data. For each subject, we calculated average time courses within each parcel of an *a priori* group average parcellation (Gordon et al., 2016) and cross-correlated those time courses to create connectivity matrices. Connectivity matrices were averages across subjects within each dataset, and participation coefficients were calculated based on the group average connectivity. As above, hubs were identified as parcels in the top 80^{th} %tile of PC values, and hubs were clustered based on the similarity of their connectivity values.

Effects of hub type removal on brain network structure

We examined how removing each hub type in turn would affect the brain's network structure. We hypothesized that removing hubs would reduce the ability of brain networks to link with each other. We evaluated this using the "path length" metric calculated using the Brain Connectivity Toolbox (Rubinov and Sporns, 2010). In each subject, path length was calculated for each network separately as the average number of node-to-node connections needed to travel between each network node and all other nodes in the brain. Disconnected nodes are traditionally assigned a path length of infinity; here, we wanted to include the disconnected nodes in the calculation, as they indicate increased network isolation. Therefore, all paths from disconnected nodes were assigned a value equal to the maximum distance between any two nodes in the brain before removing hubs. This calculation was conducted on binarized connectivity matrices thresholded at multiple graph densities ranging from 0.3% to 5% (as in "Hub Identification" above), and path lengths were averaged across thresholds for each network.

Removing nodes from a network will inevitably increase path lengths (as possible shorter connection paths are removed but are never added). Therefore, as an appropriate control, we compared the path lengths calculated for each network after removing hub nodes against path lengths calculated after removing the same number of randomly chosen non-hub nodes. Each random node was selected to be approximately matched in degree (+/− 5%tile) to a hub node. Random node selection was iterated 100 times, and resulting path lengths were averaged across iterations. For each network, comparisons between path lengths after hub removal and path lengths after random removal were conducted across subjects using paired one-tailed t tests. Significance tests were Bonferroni-corrected for the number of networks (15) and hub types (3) tested, resulting in a corrected p threshold of 0.0022.

We also explored how path lengths in each network progressively increased as more and more hubs in each category were removed. The procedure above was repeated, but instead of removing all hub nodes in a category, we removed the hubs in that category with the top 10% of PC values. Resulting path lengths calculated after this removal were compared to removal of 100 iterations of the same number of degree-matched non-hubs, as above. We then repeated this analysis removing the top 20% of PC values, the top 30%, etc, obtaining path lengths after removal of hubs with all cumulative deciles of PC values, as well as degree-matched non-hub nodes.

Effect of hub type on task activation

We hypothesized that the identity (type) of a hub region would also explain additional, unrelated variance in task activation, above and beyond that explained by differences among brain networks. To test this hypothesis, we first calculated the average task activation within each hub parcel for a number of different task contrasts. In the MSC data, these contrasts included 1) the average of all motor conditions (left hand + right hand + left foot + right foot + tongue) versus baseline in the motor task; 2) the average of both trial conditions (Glass pattern discrimination + noun/verb judgment) versus baseline in the mixed task; and 3) the average of the first and third stimulus presentations in the implicit memory task, across all stimulus types. For each task contrast, hub parcel average activations from all subjects were entered into a 3-way mixed ANOVA testing for effects of 1) network identity and 2) hub type, while controlling for 3) subject identity as a random effect of no interest.

For a more detailed examination of condition-specific effects, we repeated the above analysis for the following conditions: 1) Tongue movement versus baseline in the Motor task; 2) Left hand movement versus baseline in the Motor task; 3) Right hand movement versus baseline in the Motor task; 4) Left leg movement versus baseline in the Motor task; 5) Right leg movement versus baseline in the Motor task; 6) Glass pattern dot motion discrimination in the Mixed perceptual/language task; 7) Semantic judgment in the Mixed perceptual/language task; 8) Face stimuli in the Implicit Memory task; 9) Scene stimuli in the Implicit Memory task; and 10) Word stimuli in the Implicit Memory task.

To specifically investigate the effect of different hub types on task activation within control networks, we repeated the above ANOVAs, restricting the analysis to hubs identified as belonging to the Fronto-Parietal, Cingulo-Opercular, and Dorsal Attention networks.

To validate these findings, we replicated these analyses in the HCP data. Task contrasts used were: 1) The ''Faces'' condition versus baseline, in the Emotion task; 2) the ''Reward'' condition versus baseline in the Gambling task; 3) the ''Math'' condition versus baseline in the Language task; 4) the ''Story'' condition versus baseline in the Language task; 5) the average of all motor conditions (left hand + right hand + left foot + right foot + tongue) versus baseline in the Motor task; 6) the ''Relational'' condition versus baseline in the Relational Reasoning task; 7) the ''Theory of Mind'' condition versus baseline in the Social task; and 8) the ''2-Back'' condition versus baseline in the Working Memory task.

All significance tests were Bonferroni-corrected for the total number of tasks tested in MSC and HCP datasets, resulting in a corrected p threshold of 0.0045.

DATA AND SOFTWARE AVAILABILITY

Raw MRI data, as well as segmented cortical surfaces, preprocessed volumetric and cifti-space RSFC and task time courses, and subject-specific parcellations and networks, have been deposited in the Openneuro data repository (https://openneuro.org/datasets/ds000224/versions/00002).

Code to perform preprocessing and analysis is available at https://github.com/MidnightScanClub.

The accession number for the MSC data reported in this paper is Openneuro: ds000224.

Cell Reports, Volume *24*

Supplemental Information

Three Distinct Sets of Connector Hubs Integrate Human Brain Function

Evan M. Gordon, Charles J. Lynch, Caterina Gratton, Timothy O. Laumann, Adrian W. Gilmore, Deanna J. Greene, Mario Ortega, Annie L. Nguyen, Bradley L. Schlaggar, Steven E. Petersen, Nico U.F. Dosenbach, and Steven M. Nelson

SUPPLEMENTAL INFORMATION

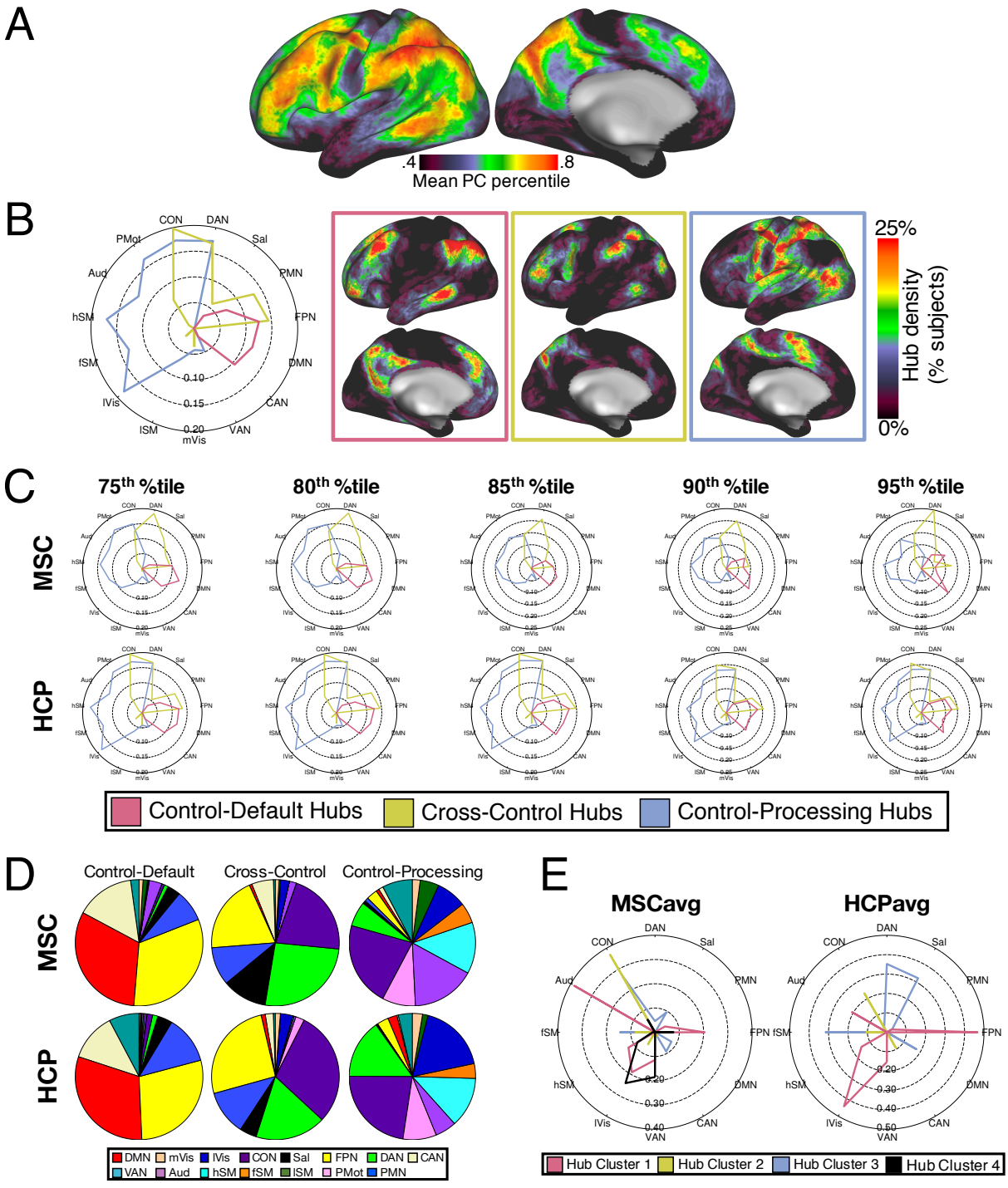

Figure S1. Related to Figure 1. A) Spatial distributions of participation coefficient (PC) values across subjects in the HCP dataset. B) Polar plots and spatial distributions for hub clusters identified in the HCP dataset. C) Polar plots illustrate the average network connectivity of each hub type in the MSC and HCP datasets at a variety of different PC percentile thresholds for hub definition. The radius of the plotted lines indicates the strength of connectivity, while the angle

of the lines indicates network. Hub type is indicated by the color of each line. D) Across MSC (top) and HCP (bottom) subjects, the average proportion of Control-Default (left), Cross-Control (middle), and Control-Processing (right) hubs within each brain network (colors). E) Clusters of hubs identified using RSFC data calculated within a priori group ROIs and averaged across MSC (left) and HCP (right) subjects. The observed clusterings were not consistent in the number of clusters generated (4 in MSC data; 3 in HCP data) or in their network connectivity patterns. Neither group average produced clusters of hubs similar to those observed in individuals. See main text for network abbreviations.

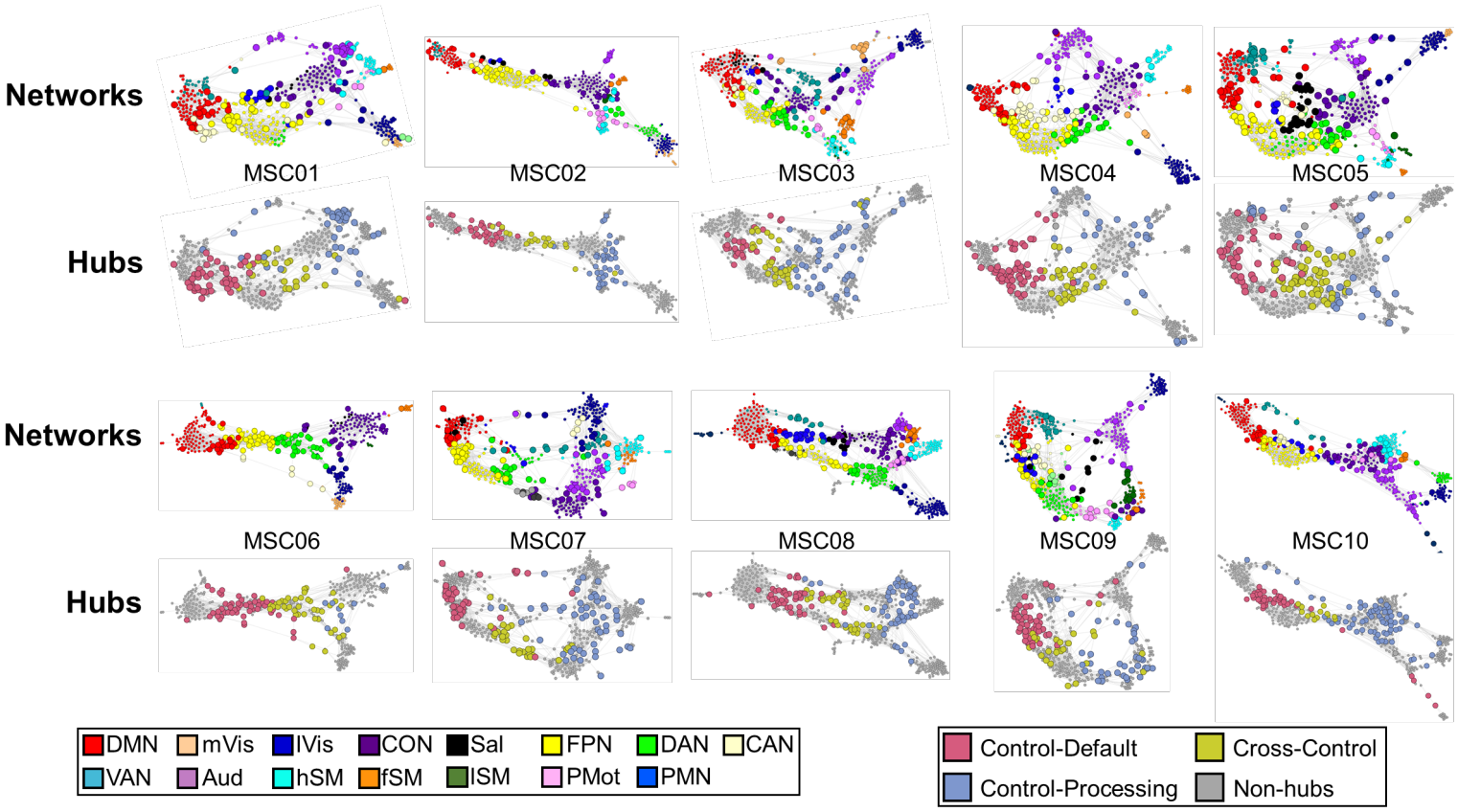

Figure S2. Related to Figure 2. Spring embedding plots showing whole-brain network structure for each MSC subject, with nodes colored by network identity (top) and hub type (bottom). See main text for network abbreviations.

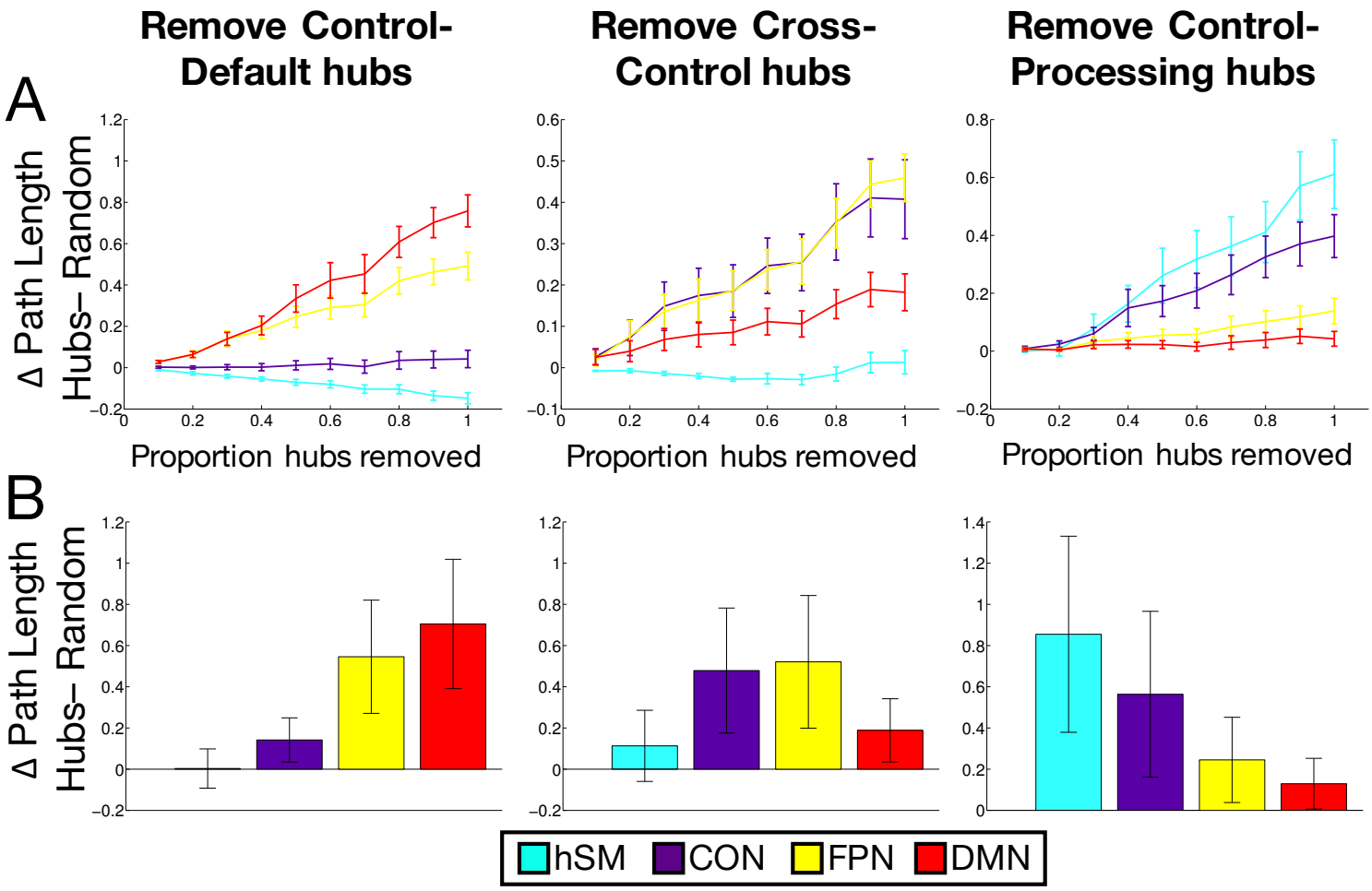

Figure S3. Related to Figure 3. A) Removal of increasing numbers of connector hub regions progressively increases path lengths in specific networks. Connector hubs of each type were progressively removed from each individual's brain network (x-axes), and average path lengths were calculated for each network and compared to path lengths after removal of an equal number of random degree-matched non-hubs (y-axes). These effects are shown for removal of Control-Default hubs (left), removal of Cross-Control hubs (middle), and removal of Control-Processing hubs (right). Across subjects, removing increasing numbers of Control-Default hubs progressively increased path lengths in DMN and FPN (left); removing Cross-Control hubs progressively increased path lengths in FPN and CON (middle); and removing Control-Processing hubs progressively increased path lengths for hSM and CON. B) Bar graphs show the difference in average path length between removing all hubs of a certain type and removing the same number of randomly selected nodes, calculated in the HCP dataset. These effects are shown for removal of Control-Default hubs (left), removal of Cross-Control hubs (middle), and removal of Control-Processing hubs (right). Results suggest that Internal hub removal preferentially affects FP and DMN networks; Control hub removal affects CON and FP networks; and External hub removal affects SMh and CON networks. See main text for network abbreviations.

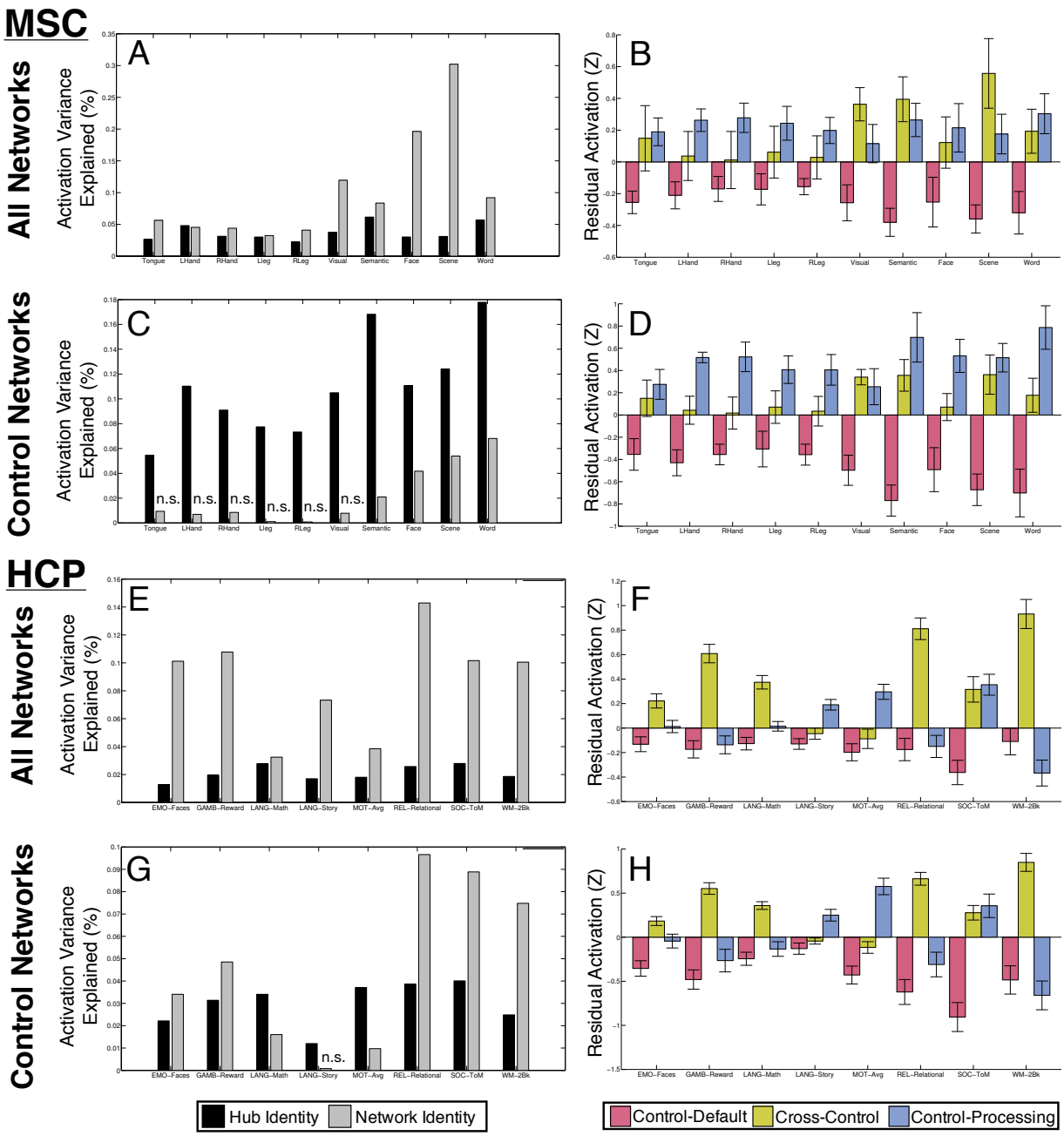
MSC
All Networks
Control Networks
HCP
All Networks
Control Networks
A
B
C
D
E
F
G
H
Activation Variance Explained (%)
Residual Activation (Z)
n.s.
Tongue
LHand
RHand
Lleg
RLeg
Visual
Semantic
Face
Scene
Word
EMO–Faces
GAMB–Reward
LANG–Math
LANG–Story
MOT–Avg
REL–Relational
SOC–ToM
WM–2Bk
Hub Identity
Network Identity
Control-Default
Cross-Control
Control-Processing

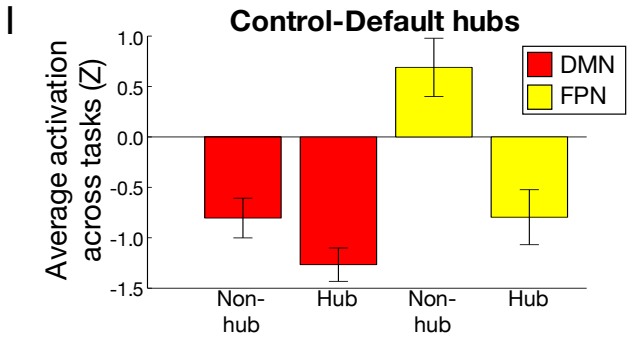
I
Control-Default hubs
Average activation across tasks (Z)
DMN
FPN
Non-hub
Hub
Non-hub
Hub

Figure S4: Related to Figure 4. A, C, E, G: Variance in task activation in the MSC (A,C) and HCP (E, G) datasets explained by hub type and by network identity across different task conditions (x-axis), within all hubs (A, E) and within just hubs in control networks (DAN, CON, FP) (C, G). All effects are significant after correction for multiple comparisons except where indicated (n.s.). B, D, F, H: Residual task activations (after controlling for subject identity and network identity) in the MSC (B, D) and HCP (F, H) datasets for each set of hubs, across different task conditions (x-axis), within all hubs (B, F) and within just hubs in control networks (D, H). I) Average activation of Control-Default hubs and non-hubs within DMN and FP. When activation levels were averaged across all task conditions, Control-Default hubs demonstrated greater deactivation than non-hubs in the same network. Error bars represent SEM across subjects.

	Control-Default	Cross-Control	Control-Processing
DMN	T=10.3, p<.001	T=4.0, p=.07	T=1.9, p>.5
VAN	T=2.1, p>.5	T=1.3, p>.5	T=2.2, p>.5
CAN	T=3.7, p=.14	T=3.3, p=.24	T=0.8, p>.5
PMN	T=2.4, p>.5	T=2.5, p>.5	T=1.2, p>.5
FPN	T=7.6, p<.001	T=7.9, p<.001	T=3.2, p=.24
Sal	T=1.1, p>.5	T=3.9, p=.14	T=2.3, p>.5
DAN	T=3.3, p=.20	T=3.6, p=.14	T=3.9, p=.08
CON	T=0.9, p>.5	T=4.4, p=.04	T=5.4, p<.01
PMot	T=-0.8, p>.5	T=3.0, p=.32	T=4.2, p=.052
Aud	T=-0.9, p>.5	T=21, p>.5	T=4.9, p=.02
hSM	T=-5.4, p>.5	T=0.7, p>.5	T=5.4, p=.009
fSM	T=-3.4, p>.5	T=0.7, p>.5	T=3.5, p=.16
lSM	T=-2.6, p>.5	T=-1.4, p>.5	T=2.2, p>.5
lVis	T=-1.9, p>.5	T=2.1, p>.5	T=4.2, p=.049
mVis	T=-1.8, p>.5	T=1.5, p>.5	T=1.5, p>.5

Table S1. Related to Figure 3. One-sided T-statistics and significance values (corrected for multiple comparisons) for the comparisons of path length after removal of each type of hub against removal of the same number of randomly selected nodes, in each network. See main text for network abbreviations.